A Decoupled CHT Procedure: Application and Validation on a Gas Turbine Vane with Different Cooling Configurations

Available online at www.sciencedirect.com

ScienceDirect

Energy Procedia 45 (2014) 1087 – 1096

Energy Procedia

68th Conference of the Italian Thermal Machines Engineering Association, ATI2013

A decoupled CHT procedure: application and validation on a gas turbine vane with different cooling configurations

Luca Andrei[a], Antonio Andreini[a], Bruno Facchini[a], Lorenzo Winchler[a,*]

[a]*Department of Industrial Engineering, University of Florence, via di Santa Marta 3 - 50139, Florence, Italy*

Abstract

Gas turbine performance improvement is strictly linked to the attainment of higher maximum temperature, hence heat load management becomes an essential activity.

This paper presents a decoupled procedure aimed to predict cooling performances and metal temperatures of gas turbine blades and nozzles: needed inputs are evaluated by different tools (CFD, in-house fluid network solver, thermal FEM). The procedure is validated on two different test cases: an internally cooled vane (Hylton et al.[1]), and an internally and film cooled vane (Hylton et al.[2]). Metal temperature and adiabatic effectiveness distributions are compared against experimental data and results from a fully 3D coupled CHT CFD analysis.

Selection and peer-review under responsibility of ATI NAZIONALE

Keywords: gas turbine; heat transfer; decoupled procedure; CHT; fluid network solver; film cooling; C3X.

1. Introduction

In order to improve gas turbines performances, in terms of higher thermodynamic efficiency and power output, combustor exit temperature levels must be increased and coolant flow rate reduced. An accurate assessment of thermal load is the key to correctly predict the life of the hot gas path components. Gas turbine blades can be considered as ones of the most critical components due to their exposure to high thermal and centrifugal loads. Considering that small variations of blade temperature can lead to a strong reduction of blade lifespan, accurate numerical methods and tools are required. Hence, it is necessary to consider both fluid-dynamic and thermal conduction phenomena. The Conjugate Heat Transfer (CHT) analysis can be accounted as an indispensable tool to improve the performance and reliability of the gas turbine engine.

Conjugate procedures can be classified into two main categories, depending on the method used to solve the specific equation set of the problem: *Coupled Approach* and *Decoupled* (or *Segregated*) *Approach*. The former consists of the simultaneous solution of the equation set which characterizes different fields. The great advantage of this method is that the coupling interfaces become part of the solution domain so that continuity of the temperature and heat flux at the interfaces is implicitly guaranteed, although this approach may lead to a difficult convergence (Zhenfeng et al.[3]).

* Corresponding author. Tel.: +39-055-479-6618 ; fax: +39-055-479-6342.
E-mail address: lorenzo.winchler@htc.de.unifi.it

1876-6102
Selection and peer-review under responsibility of ATI NAZIONALE
doi:10.1016/j.egypro.2014.01.114

In the *Decoupled Approach* each field is solved separately to provide boundary conditions for the other ones, therefore an exchange of information at the interface of the contiguous domains becomes necessary. Since both internal and external heat transfer deeply depends on the wall temperature, an iterative procedure is hence necessary to ensure the continuity of temperature and heat fluxes at the fluid-solid interface. So, in each iteration the heat transfer coefficients and film effectiveness are computed assuming a fixed wall temperature distribution.

Several works dealing with Conjugate Heat Transfer (CHT) problems on gas turbine components can be found in literature. Bohn et al.[4,5] described their Conjugate Calculation Technique (CCT) applied to gas turbine vanes and blades. Takahashi et al.[6] applied conjugate analysis of heat transfer inside and outside a first rotor blade of a gas turbine to predict the metal temperature. Heidmann et al.[7] simulated the three-dimensional coupled internal/external flow-field of a realistic film cooled turbine blade. Li and Kassab[8,9], Kassab et al.[10] proposed an alternative approach that couples fluid and thermal solutions combining Finite Volume Method (FVM) approach to solve fluid domain and Boundary Element Method (BEM) to solve solid conduction. In conclusion, most CHT methods are based on Finite Volume Method, Finite Element Method and Boundary Element Method or by combinations of them.

Since a decoupled approach allows to choose the best method for solving each domain, an interesting solution can be the use of one-dimensional thermo-fluid network approach in order to solve the internal fluid cooling system. Use of one-dimensional models for solving fluid network elements represents an accurate and robust design tool for evaluating global parameters (like pressure losses or heat transfer coefficient) if these models refer to a robust set of commonly used best-practice correlations. This kind of approach allows sensitivity analyses, especially for preliminary considerations or optimization strategies, due to the reduced calculation time. Jelisavcic et al.[11],Martin and Dulikravich[12] used a fluid network approach to perform a multidisciplinary optimization of internal cooling passages. Carcasci and Facchini[13], Carcasci et al.[14] performed a blade-to-blade thermal analysis of a PGT10 rotor blade and a vane of PGT2 gas turbine. Zecchi et al.[15] showed the reliability of a preliminary design stage procedure involving a fluid network approach performing a CHT analysis of NASA C3X test case. None of the cited works however can be accurately used to predict the full 3D metal temperature distribution of a blade, being mainly conceived for the optimization of internal cooling geometry or based on 2D conductive solutions.

An iterative procedure developed to solve a conjugate heat transfer problem in a decoupled way was recently presented by Andreini et al.[16,17]: this methodology has been applied on a first rotor blade of a heavy duty gas turbine. In this methodology the internal cooling system is modelled by an in-house one-dimensional thermo-fluid network solver, external heat loads and pressure distributions are evaluated through 3D CFD and heat conduction through the solid is computed through a 3D FEM solution. The proposed methodology is placed in the middle between fully 3D CFD tools, that require a complete meshing of the cooling system, and classical fluid network-based tools coupled with simplified conductive models. It allows, in fact, to contain computational costs, mainly related to CFD discretization of cooling features, obtaining nevertheless results with an adequate overall accuracy. This characteristic is the main innovative nature of the new procedure, assuring its feasibility in both preliminary and detailed design phases.

The aim of this work is to validate and compare the above mentioned decoupled procedure under different cooling scheme configurations against experimental data and fully coupled CHT simulation. Two typical blade cooling schemes have been considered: one employs ten internal radial cooling channels and the other one adds showerhead and film cooling rows to the previous configuration. Comparisons are presented in terms of metal temperature, airfoil static pressure and adiabatic effectiveness profiles.

Nomenclature

Ax_{Ch}	Axial chord $[m]$	P	Pressure $[Pa]$
D	Diameter $[m]$	Pr	Prandtl number $[-]$
f	Friction factor $[-]$	$\dot{q}$	Wall heat flux $[W/m^2]$
HTC	Heat transfer coefficient $[W/m^2K]$	Re	Reynolds number $[-]$
k	Thermal conductivity $[W/mK]$	T	Temperature $[K]$
$\dot{m}$	Mass flow $[kg/s]$	X	Axial coordinate $[m]$
L	Length $[m]$	y^+	Dimensionless wall distance$[-]$

Acronyms

LE	Leading Edge	SS	Suction Side
PS	Pressure Side		

Greeks

η_{aw}	Adiabatic effectiveness

Subscripts and Superscripts

aw	Adiabatic wall	ref	Reference
eq	Equivalent	s	Static
ext	External	t	Total
int	Internal	w	Wall

2. CHT decoupled procedure

The procedure, presented in this paper, is able to perform conjugate heat transfer analysis of gas turbine blades and nozzles in a decoupled way. The interactions between various solvers, each one solving a specific part of the conjugate heat transfer analysis, are ruled by *ad hoc* tools. The simplified block diagram in Figure 1 shows the main solvers and tools involved in the procedure. Some features of the procedure are presented below. For a more detailed description, the reader is referred to [16] and [18].

2.1. 1D Fluid Network Solver (SRBC)

The internal cooling system is modelled using an in-house developed one-dimensional steady state fluid network solver in which the most common cooling techniques and patterns are implemented. The heat transfer coefficient and the pressure losses of each model representing a cooling system is evaluated by a set of correlations collected in literature during years. Further details about the solver can be found in [14] and [13].

2.2. 3D CFD

External thermal loads and pressure distribution are provided by dedicated 3D CFD computations. The decoupled nature of the presented *CHT* procedure involves the use of HTC and T_{aw} to express external loads on blade surface and an external static pressure field as input for the fluid network solver to obtain the right β for each film cooling hole.

The role played by CFD analysis inside the decoupled procedure is limited to:

- an adiabatic simulation to provide T_{aw} and $p_{s,ext}$;
- a fixed wall temperature simulation for each overall iteration to provide HTC_{ext} values.

At each iteration of the overall procedure, the fixed wall temperature simulation is carried out using the most updated wall metal temperature distribution as input. Therefore, in order to keep a consistent definition of HTC

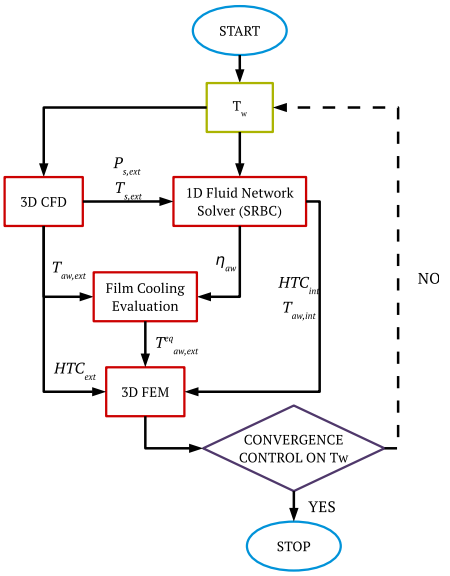

Fig. 1: Block diagram of the iterative decoupled procedure.

despite the local values of adiabatic wall temperature, affected by the mixing with purge flows, the expression used is:

$$HTC_{ext} = \frac{\dot{q}}{(T_{aw} - T_w)} \tag{1}$$

where $\dot{q}$ is the wall heat flux, T_{aw} (the adiabatic wall temperature obtained from the adiabatic simulation) is the reference temperature value and T_w is the wall temperature. Such definition of HTC_{ext} is chosen with the purpose of avoiding an equation denominator value equal to 0.

The effect of coolant film, in terms of T_{aw}, is computed through specific correlations (as explained in the following section).

2.3. Film cooling and holes heat sink effect

The film cooling effect is evaluated from the fluid network solver by computing, along prearranged radial sections of the blade, the adiabatic effectiveness using the L'Ecuyer and Soechting[19] correlation for cylindrical holes and the correlation proposed by Colban et al.[20] for shaped holes: film superposition is handled by the formula proposed by Sellers[21]. Local external conditions required as input by the correlations (pressure, gas velocity and temperature), are obtained from the adiabatic CFD simulation. The resulting distribution of adiabatic film effectiveness is then interpolated on the 3D surface of the airfoil and local values of adiabatic wall temperature (T_{aw}), predicted by the CFD simulation, are corrected according to the definition of adiabatic effectiveness:

$$T^{eq}_{aw,ext} = T_{aw} - \eta_{aw}(T_{aw} - T_c) \tag{2}$$

where η_{aw} is the local value of adiabatic effectiveness after the interpolation from the correlation data and T_c the coolant temperature exiting from each hole (computed by the fluid network solver).

The heat removal due to convection through the film cooling holes has been taken into account considering the Dittus Boelter convection correlation coupled to a correction to handle the effect of length-to-diameter ratio below 10 [22]. This approach allows to avoid film cooling holes meshing, strongly reducing the computational costs.

2.4. FEM 3D Thermal conduction model

Finally, once external and internal thermal loads are computed, conduction through the metal of the blade can be solved. The procedure uses the FEM module of ANSYS® v.14. External load values (HTC_{ext} and $T^{eq}_{aw,ext}$), obtained by CFD and film cooling steps, are interpolated on external blade surfaces of FEM mesh (airfoil, endwalls). In the same way internal loads coming from the fluid network solver, in terms of HTC and T_{aw}, are interpolated on the internal cavities of the blade. The entire set of interpolation steps is completely managed by automated tools coupled with the ANSYS® Workbench environment. FEM grid is clustered enough to limit discretization errors due to interpolation process on non-conformal grids.

2.5. Convergence criteria

The convergence is verified checking computed wall metal temperature on each mesh node. The procedure convergence is assessed when relative errors between the last two iterations is below 0.1%. Usually less than 10 iterations are required to get convergence.

3. Internally cooled vane (*C3X-1983*)

3.1. Description of test case

The first analysed cooling configuration is the one related to the well known NASA test case, called *C3X-1983*, originally presented by Hylton et al.[1]. The test case is representative of a highly loaded, low solidity airfoil, simulated at engine conditions. The vane is internally cooled by an array of 10 radial cooling holes (Figure 2a).

3.2. Boundary conditions

Boundary conditions of the particular case chosen for this simulation are retrieved from Hylton et al.[1]: the case is named *code 4422*, *run 112*. Definitive values of total inlet temperatures imposed on cooling channel inlets were found via an iterative process aimed at matching, for each channel, experimental mass averaged static temperature [23]. In addition, the total inlet pressure values for each tube, imposed as a boundary for the fluid network solver, were evaluated following an another iterative process in order to match the experimental mass flow rate and the outlet static pressure.

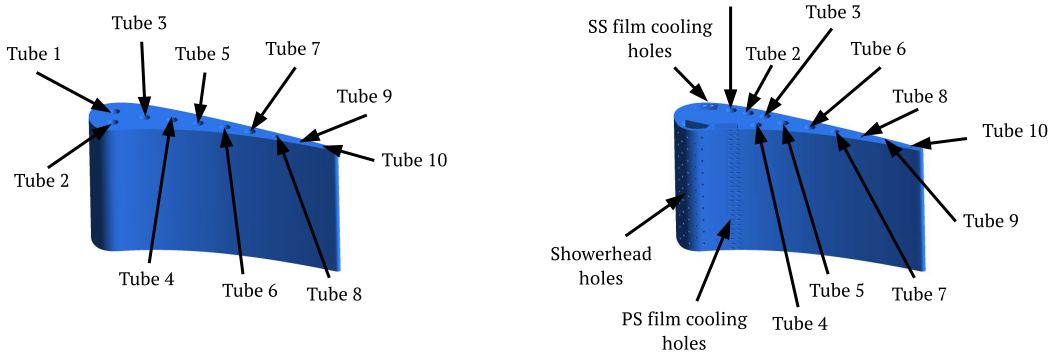

(a) Internally cooled geometry (*C3X-1983*). (b) Internally and film cooled geometry (*C3X-1988*).

Fig. 2: Studied geometries.

3.3. Numerical setup

3.3.1. Procedure-supporting CFD simulations

Steady-state CFD RANS calculations have been performed with the commercial 3D Navier-Stokes solver ANSYS® CFX v14. In Figure 3, the numerical domain is reported. The flow path boundary conditions have been recovered from Hylton et al.[1]: total pressure, total temperature, turbulence intensity ad length scale values at the inlet; while at the outlet, static pressure value is applied.

Compressibility effects have been taken into account and the High Resolution advection scheme has been used. The fluid has been modelled as ideal gas and the properties of specific heat capacity, thermal conductivity and viscosity were expressed as function of temperature. Energy equation has been solved in terms of total energy and viscous heating effects have been accounted for. The $k-\omega$ SST turbulence model, in its formulation made available by the CFD solver, has been used in conjunction with an automatic near-wall treatment approach. Transition from laminar to turbulent boundary layer has been taken into account employing the $\gamma-\theta$ model available in ANSYS® CFX v14 (this choice is driven by a transition model sensitivity analysis against experimental data, here not reported).

The solution convergence has been assessed by monitoring the residuals. Numerical grid is the same employed by [23]: a 7.3×10^5 elements hexahedral grid (with a y^+ on the blade below 0.5).

3.4. FEM setup

The conduction through the metal of the blade is solved by the three-dimensional Fourier's law solver module of ANSYS® v14 (*Steady-State Thermal Module*). The boundary conditions are both the internal and external thermal loads derived from the CFD and from the fluid network solver appropriately interpolated on the surfaces of the blade. The value of thermal conductivity was specified to vary linearly with the temperature as reported by Facchini et al.[23]:

$$k(T) = 6.811 + 0.020176 \cdot T \tag{3}$$

The numerical grid consists of about 6.0×10^5 tetrahedral elements (with ten nodes).

4. Internally and film cooled vane (*C3X-1988*)

4.1. Description of test case

The second studied test case is the one presented by Hylton et al.[2], exploiting the same vane geometry described previously, but with a different cooling scheme (Figure 2b). The test vane is internally cooled by the introduction of an array of 10 radial tubes, and externally cooled by film cooling. The film cooling scheme consists of holes array on the leading edge, on the suction side and on the pressure side. The leading edge array employed a showerhead array of five equally spaced and staggered holes.

The vane presents a thermal barrier separating the leading edge and the tail region (Figure 2b). All the geometry characteristics of the vane have been recovered from Hylton et al.[2].

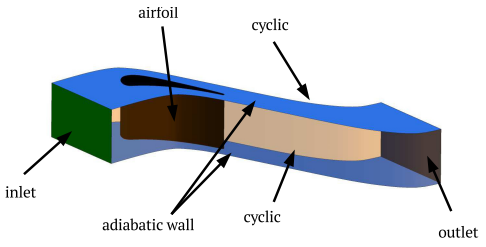

Fig. 3: CFD domain of procedure-supporting simulations.

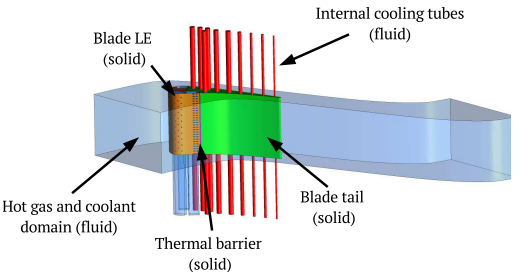

Fig. 4: *C3X-1988* conjugate analysis numerical domain.

4.2. Boundary conditions

Coolant supply conditions for the ten channels were not documented in the original report [2] and the literature is poor about this information. Laskowski et al.[24] in their work present an inverse procedure for finding the mass flow rate and the total inlet temperature for each channel in order to match the experimental metal temperature distribution at midspan. They provided boundary conditions only for case *run 44344* and for this reason it is chosen for the present analysis.

4.3. Numerical setup

4.3.1. Procedure-supporting CFD simulations

In this case, the numerical domain and grid are the very same grid exploited in the procedure-supporting CFD simulations of the *C3X-1983* test case (Figure 3).

As for the previous case, compressibility effects have been taken into account and the High Resolution advection scheme has been used. The fluid has been modelled as ideal gas and the properties of specific heat capacity, thermal conductivity and viscosity were expressed as function of temperature. Energy equation has been solved in terms of total energy and viscous heating effects have been accounted for. The $k-\omega$ SST turbulence model, in its formulation made available by the CFD solver, has been used. On the other and, in this case no transitional turbulence model has been applied due to the presence of film cooling holes on the airfoil modifying the external flowpath.

The flow path boundary conditions have been recovered from Hylton et al.[2].

4.3.2. Fully 3D coupled conjugate analysis

In Figure 4, the numerical domain employed in the fully 3D coupled conjugate analysis is depicted. Following the experimental test rig configuration, the solid blade has been discretized with three different solid domains: the blade LE (where the film cooling feeding plena are placed), the blade tail (where the internal cooling tubes are located) and the insulating thermal barrier between the two solids. The fluid domain comprehend both the hot gas path flow and the three film cooling plena: in this way no interface connections between fluid domains are needed.

Moreover, in order to track the coolant distribution, four transport equations for as much additional passive scalars representing coolant concentration were solved, settings their value accordingly to the particular plenum, holding the value 1 at the particular plenum inlet and 0 at the other inlets: one passive scalar for the coolant coming from each plenum and one passive scalar (*coolant*) representing the film cooling effect of all the coolant.

Blade LE and blade tail solids employ temperature dependent proprieties (following [23]). Concerning the thermal barrier solid, a low constant thermal conductivity value ($0.03\ W\ m^{-1}\ K^{-1}$) is applied.

Numerical grid is composed by an hybrid (tetra and 20 prism layers at the solid walls) unstructured mesh. The mesh counts: 2.5×10^7 elements for the hot gas and coolant domain, 8.1×10^6 for all the solid domains and 6.0×10^6 for the internal cooling tubes domain (Figure 4).

As for the the procedure-supporting CFD simulations, the flowpath boundary conditions are recovered from [2], as for the plena boundary conditions.

As explained above, the coolant supply conditions for the ten channels were not documented in the original report [2] and they are recovered from [24].

4.4. FEM setup

As for the previous case, the conduction through the metal of the blade is solved by the *Steady-State Thermal Module* of ANSYS® v14. The boundary conditions are both the internal and external thermal loads derived from the CFD and from the fluid network solver interpolated on the blade surfaces. Thermal conductivity values of LE and tail bodies is recovered from Eq. 3, while the thermal barrier body conductivity value is the same applied in the conjugate analysis. For this simulations, the numerical grid consists of about 9.8×10^5 tetrahedral elements (with ten nodes).

5. Discussion of results

In order to assess the accuracy of the proposed procedure, comparisons with experimental metal temperature values on the midspan of the blade (as reported in [1] and [2]) will be now discussed. Furthermore, comparison with external pressure values for internally cooled vane and with adiabatic effectiveness for the film cooled vane are reported to explain the numerical results. Both temperature and pressure values were normalized with the reference values reported in [1] and [2]. Moreover, concerning T_w/T_{ref}, error bars of ±2% (as reported in [1] and [2]) are applied.

5.1. Internally cooled vane (C3X-1983)

The 1D fluid network solver allows to manually choose the convection correlation for each model of the network. Concerning the internal tubes, two different correlations have been tested: the Dittus-Boelter correlation for heating fluid [25] (*case 1*) and the Gnielinski correlation [26] (*case 2*). The values of Re, Pr and L/D are inside the range of applicability of the correlations [22]. The value of the friction factor f found in Gnielinski equation is evaluated by the fluid network solver using an internal tabular implementation of the Moody chart.

In order to validate the external flow field, a comparison of pressure values coming from the procedure-supporting CFD simulations with the experimental data [1] is presented. Airfoil HTC and T_{aw} values resulting from CFD are boundary conditions for the fluid network solver and FEM model and they are directly linked with external flow-field. Results are reported in Figure 5a as midspan profile along X/Ax_{Ch}: a good agreement can be found except for a dip right before 60% of the SS, probably due to variations of the onset point predicted by the transition model of the CFD simulation.

Figure 5b shows the comparison between experimental metal temperatures [1] and numerical values coming from the thermal procedure. Both the cases show a good agreement with the experimental data in terms of both values and trends, except on the SS due to the underprediction of external pressure values and hence of the heat transfer coefficient.

5.2. Internally and film cooled vane (C3X-1988)

As for the other cooling scheme, two simulations were carried out: one employs Dittus Boelter equation (*case 1*) and the other employs Gnielinski equation (*case 2*). A comparison with the conjugated run and experimental values [2] is reported in Figure 6a (metal temperature values on the leading edge region are not reported by Hylton et al.[2]): small differences between simulations with different convection correlations can be found. Comparison with experimental data shows a very good agreement except for small differences on the pressure side near −40% of the blade.

In Figure 6b, η_{ad} midspan values are reported: the spikes on the conjugate data are relative to the injection holes, where the coolant concentrations are equal to 1. Due to very similar η_{ad} values, only *case 1* data are reported.

In the region interested in film cooling coverage effect, strong 3D phenomena due to the interaction between jets coming out from the plena and the main flow are present. Besides, as reported above, SS and PS holes are placed just upstream the suction and pressure recovery region respectively, introducing another solid 3D effect. These phenomena could explain the difference in terms of metal temperature and adiabatic effectiveness between procedure and conjugate results. As can be seen in Figure 6b, where the midspan η_{ad} values evaluated through correlation (procedure) and conjugate CFD are reported, looking at the LE region ($-0.22 \leq X/Ax_{Ch} \leq 0.25$), a good agreement between the two numerical approaches can be seen, in terms of values and trends.

Moving toward the PS, some differences arise. In Figure 6c, the CFD coolant concentrations in a plane cutting the axes of near-midspan PS e SS holes is depicted: in particular, only the coolant coming from the two film cooling feeding plena are represented. The adverse pressure gradient on PS leads to a greater boundary layer, and a greater coolant protection predicted by conjugate analysis, resulting in metal temperature differences in Figure 6a. The *case 1* wall temperature values have a slightly worse agreement in respect to experimental data then conjugate ones. The correlative-based approach results to not be able to catch these strong 3D interactions. Going ahead towards the trailing edge, these effects softened (combining with the internally cooling effect of the tubes) leading to a very good agreement of the results.

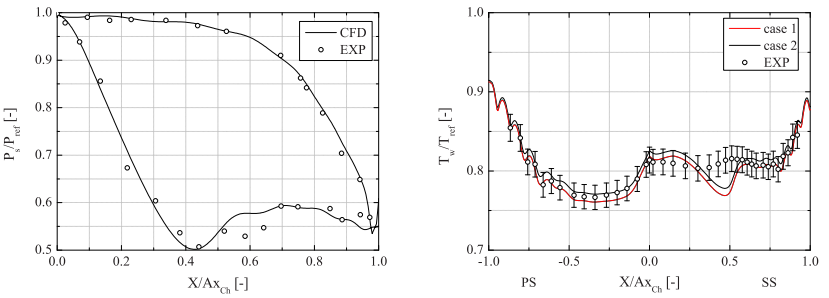

(a) Midspan airfoil static pressure. (b) Midspan wall temperature.

Fig. 5: Comparison with experimental data for the *C3X-1983 case*.

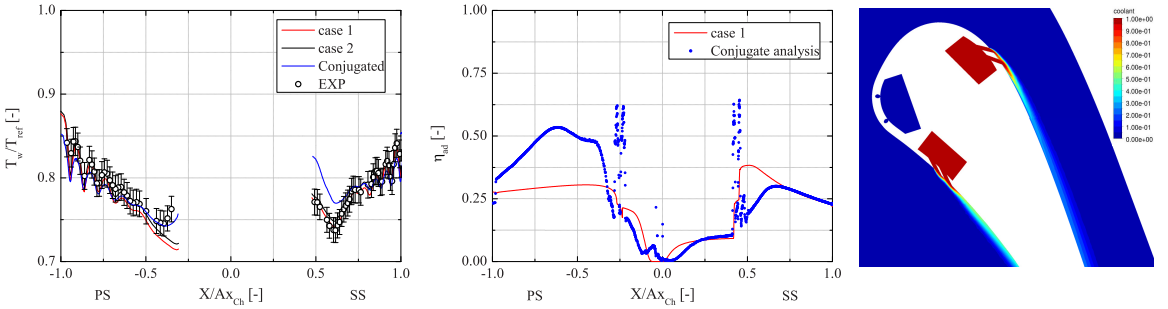

(a) Midspan metal temperature of the blade. (b) Midspan η_{ad} of the blade. (c) Injected coolant.

Fig. 6: Comparison with experimental data for the *C3X-1988 case*.

Concerning the SS, looking at the η_{ad} profiles in Figure 6b, in the region right after the coolant injection, it is possible to observe a different behaviour of the two simulations: *case 1* presents greater values of η_{ad} than conjugate predictions, leading to a better T_w/T_{ref} values agreement with experimental data.

Conjugate CFD analysis predicts jets penetration regime as can be seen in Figure 6c: this explains the differences in η_{ad} and so in metal temperatures with thermal procedure results. When jets reattach on the surface, for $X/Ax_{Ch} \geq 0.6$, the numerical agreement improves.

6. Conclusions

A decoupled procedure aimed to predict metal temperature distribution of gas turbine blades and nozzles is presented. Various inputs needed by the procedure are evaluated by different tools. Main flow temperature, pressure and heat transfer coefficient distributions are estimated by 3D CFD simulations while the internal cooling system of the blade is modelled by an in-house one-dimensional fluid network solver. The heat conduction through the solid is computed through a 3D FEM solution. Film cooling holes were treated as heat sinks while the film cooling effect is evaluated by a correlation-based approach: avoiding the discretization of film cooling holes in CFD model allows to strongly reduce the computational costs.

Both internally cooled vane and internally and film cooled vane case of NASA-C3X were studied and results were compared with experimental data. The estimated metal temperature values highlight a good agreement with measured experimental data except for some differences due to a difficult transition region prediction for the *C3X-1983* case.

C3X-1988 case was also compared with a coupled fully 3D conjugate simulation carried out to better understand the film cooling phenomena. Some differences between conjugated, thermal procedure simulations and experimental data is reported but the overall agreement is good. Main differences are to assume to the strong 3D interactions of film cooling with the main flow, difficult to predict using a correlation-based approach.

The procedure results indicate that a decoupled correlative approach can become a useful and reliable tool in gas turbine cooling analysis and design.

Acknowledgements

Part of this work was the subject of the MS Thesis discussed by Mr. Lorenzo Mazzei whose contributions are gratefully acknowledged. Authors would like to thank Miss Sabrina Giuntini for her work and for sharing her results.

References

[1] Hylton, L.D., Mihelc, M.S., Turner, E.R., Nealy, D.A., York, R.E.. Analytical and Experimental Evaluation of the Heat Transfer Distribution over the Surfaces of Turbine Vanes. NASA CR-168015; 1983.
[2] Hylton, L.D., Nirmalan, N.V., Sultanian, B.K., Kaufman, R.M.. The Effects of Leading Edge and Downstream Film Cooling on Turbine Vane Heat Transfer. NASA CR-182133; 1988.
[3] Zhenfeng, W., Hongyan, H., Peigang, Y., Wanjin, H.. Coupled BEM and FDM conjugate analysis of a three-dimensional air-cooled turbine vane. Proceedings of ASME Turbo Expo 2009;GT2009-59030.
[4] Bohn, D., Bonhoff, B., Schönenborn, H., Wilhelmi, H.. Validation of a numerical model for the coupled simulation of fluid flow and diabatic walls with application to film-cooled gas turbine blades. VDI-Berichte 1995;1186:259–272.
[5] Bohn, D., Bonhoff, B., Schönenborn, H.. Combined aerodynamic and thermal analysis of a high-pressure turbine nozzle guide vane. Proceedings of IGTC 1995;108:I–35–I–39.
[6] Takahashi, T., Watanabe, K., Takahashi, T.. Thermal conjugate analysis of a first stage blade in a gas turbine. Proceedings of ASME Turbo Expo 2000;GT2000-0251.
[7] Heidmann, J.D., Kassab, A.J., Divo, E.A., Rodriguez, F., Steinthorsson, E.. Conjugate heat transfer effects on a realistic film-cooled turbine vane. Proceedings of ASME Turbo Expo 2003;GT2003-38553.
[8] Li, H.J., Kassab, A.J.. Numerical prediction of fluid flow and heat transfer in turbine blades with internal cooling. AIAA, ASME, SAE, and ASEE, Joint Propulsion Conference and Exhibit 1994;(2933).
[9] Li, H.J., Kassab, A.J.. A coupled FVM/BEM solution to conjugate heat transfer in turbine blade. AIAA Paper 1994;(94-1981).
[10] Kassab, A.J., Divo, E., Heidmann, J.D.. BEM/FVM conjugate heat transfer analysis of a three-dimensional film cooled turbine blade. International Journal of Numerical Methods in Heat Transfer and Fluid Flow 2003;13(5):581–610.
[11] Jelisavcic, N., Moral, R.J., Dulikravich, G.S., Martin, T.J., Sahoo, D., Gonzalez, M.. Design optimization of networks of cooling passages. Proceedings of ASME IMECE 2005;IMECE2005-79175.
[12] Martin, T.J., Dulikravich, G.S.. Analysis and multidisciplinary optimization of internal coolant networks in turbine blades. Journal of Propulsion and Power 2002;18(4):896–906.
[13] Carcasci, C., Facchini, B.. A numerical procedure to design internal cooling of gas turbine stator blades. Revue Générale de Thermique 1996;35:257–268.
[14] Carcasci, C., Facchini, B., Ferrara, G.. A rotor blade cooling design method for heavy duty gas turbine applications. ASME Cogen-turbo Power Conference 1995;95-CTP-90:1–8.
[15] Zecchi, S., Arcangeli, L., Facchini, B., Coutandin, D.. Features of a cooling system simulation tool used in industrial preliminary design stage. Proceedings of ASME Turbo Expo 2004;GT2004-41685:493–501.
[16] Andreini, A., Bonini, A., Carcasci, C., Facchini, B., Innocenti, L., Ciani, A.. Conjugate heat transfer calculations on GT rotor blade for industrial applications. Part I: equivalent internal fluid network setup. Proceedings of ASME Turbo Expo 2012;GT2012-69846.
[17] Andreini, A., Bonini, A., Soghe, R.D., Facchini, B., Ciani, A., Innocenti, L.. Conjugate heat transfer calculations on GT rotor blade for industrial applications. Part II: improvement of external flow modeling. Proceedings of ASME Turbo Expo 2012;GT2012-69849.
[18] Andrei, L., Andreini, A., Bonini, A., Soghe, R.D., Facchini, B., Mazzei, L., et al. CHT analyses of an industrial gas turbine blade: Comparison between an in-house developed decoupled procedure and cfd coupled simulations. Proceedings of 10th European Turbomachinery Conference 2013;.
[19] L'Ecuyer, M.R., Soechting, F.O.. A model for correlating flat plate film cooling effectiveness for rows of round holes. AGARD Conference Proceedings No 390, Heat Transfer and Cooling in Gas Turbines 1985;19.
[20] Colban, W.F., Thole, K.A., Bogard, D.. A film-cooling correlation for shaped holes on a flat-plate surface. ASME J Turbomach 2011;133:1–11.
[21] Sellers, J.P.. Gaseous film cooling with multiple injection stations. AIAA Journal 1963;1:2154–2156.
[22] Bergman, T.L., Lavine, A.S., Incropera, F.P., Dewitt, D.P.. Fundamentals of Heat and Mass Transfer. 7th Edition; 2011.
[23] Facchini, B., Magi, A., Greco, A.S.D.. Conjugate heat transfer simulation of a radially cooled gas turbine vane. Proceedings of ASME Turbo Expo 2004;(GT2004-54213).
[24] Laskowski, G.M., Ledezma, A.G., Tolpadi, A.K., Ostrowsky, M.. Cfd simulations and conjugate heat transfer analysis of a high pressure turbine vane utilizing different cooling configurations. 12th ISROMAC Symposium, 17-22 February 2008, Honolulu, Hawaii 2008;*ISROMAC*12-2008-20065.
[25] Winterton, R.H.S.. Where did the dittus and boelter equation come from? International Journal of Heat and Mass Transfer 1998;41.
[26] Gnielinski, V.. New equations for heat and mass transfer in turbulent pipe and channel flow. International Chemical Engineering 1976;16.